Modeling the corneal birefringence of the eye toward the development of a polarimetric glucose sensor

Bilal H. Malik
Gerard L. Coté
Texas A&M University
Department of Biomedical Engineering
337 Zachry Engineering Center, 3120 TAMU
College Station, Texas 77843-3120

Abstract. Optical polarimetry for monitoring glucose concentration in the aqueous humor of the eye as a potential noninvasive means of assessing blood glucose has promise, but the realization of such an approach has been limited by noise from time-varying corneal birefringence due to motion artifact. Modeling the corneal birefringence of the eye is critically important toward understanding the overall effect of this noise source compared to other changes in the signal, and can aid in design of the polarimetric system. To this end, an eye model is introduced in this work that includes spatially varying birefringence properties of the cornea. The degree of birefringence and the fast axis orientation is calculated as a function of beam position on the anterior chamber. It is shown that the minimum change in polarization vector orientation occurs for beam position near the midpoint between the corneal apex and limbus. In addition, the relative wavelength independence of motion artifact is shown in the same region. The direct consequence of these findings are that a multiwavelength polarimetric system can potentially be utilized to eliminate the effect of time-varying corneal birefringence, and that eye coupling is optimal at the midpoint between the apex and limbus. [DOI: 10.1117/1.3447923]

Keywords: optical polarimetry; glucose sensing; corneal birefringence; dual wavelength; noninvasive; motion artifact.

Paper 10108R received Mar. 4, 2010; revised manuscript received Apr. 21, 2010; accepted for publication Apr. 22, 2010; published online Jun. 15, 2010.

1 Introduction

Optical polarimetric quantification of glucose is based on the phenomenon of optical activity, which is the ability of glucose molecules to rotate the plane of polarization of the transmitted linearly polarized light in direct proportion to the concentration of the glucose. One of the difficulties associated with utilizing polarimetry for glucose sensing *in vivo* is that most biological tissues are optically turbid. Polarimetric sensing of glucose in such media thus becomes challenging due to multiple scattering events, which scramble the potentially useful information encoded in the state of polarization of the reflected or transmitted light. A possible way to overcome these problems is to probe the anterior chamber of the eye, since the absorption effects are minimal, loss of polarization information due to scattering effects is insignificant, glucose is the principal chiral component, and a direct correlation exists between blood glucose concentration and that of aqueous humor.[1]

Several research groups have demonstrated the application of optical polarimetry to glucose sensing *in vitro* with acceptable repeatability of less than 15-mg/dl standard error.[2–5] In contrast, the *in vivo* performance of this technique has been limited primarily by the inherent time-varying birefringence of cornea due to motion artifact, which makes it difficult to discern the rotation due to glucose.[6] The cornea changes the state of polarization of the transmitted beam due to the structure of corneal stroma, which mainly consists of collagen lamellae.[7–9] Each lamella exhibits intrinsic birefringence and can be considered a linear retarder with the fast axis perpendicular to the fibril orientation. The total corneal birefringence manifests itself as form birefringence, and can be considered as the sum of individual lamella birefringence.

The typical equation describing the rotation of plane of polarization of light as a function of glucose is given by:

$$\alpha = [\alpha]_\lambda C \cdot L, \tag{1}$$

where α is the observed rotation, C is the concentration of the optically active sample, and L is the sample path length. In this equation, $[\alpha]$ is the specific rotation dependent on wavelength (λ). This dependence is known as optical rotatory dispersion and is further defined using the modified Drude equation for wavelengths away from or between the absorption bands, namely,[10]

$$[\alpha]_\lambda = \frac{k_o}{\lambda^2 - \lambda_o^2}, \tag{2}$$

where λ is the wavelength of interest, and k_o is a rotational constant corresponding to the wavelength λ_o of maximal ab-

Address all correspondence to: Bilal H. Malik, Department of Biomedical Engineering, Texas A&M University, 337 Zachry Engineering Center, 3120 TAMU, College Station, TX 77843-3120. Tel: 979-862-1076; Fax: 979-845-4450; E-mail: malik@tamu.edu

1083-3668/2010/15(3)/037012/6/$25.00 © 2010 SPIE

sorption. For glucose, the values of k_o and λ_o are 16.74 deg and 0.17236 μm, respectively. Although Eqs. (1) and (2) describe the relationship between glucose concentration, optical path length, the rotation in the plane of light polarization, and the specific rotation as a function of wavelength in a clear optical media, neither equation takes into account the effect of birefringence such as that found in the cornea. Further, although two methods have been proposed to accommodate time-varying birefringence noise,[5,11] there has been no quantifiable estimate of this noise as a function of position along the cornea. The first method proposed by our group to accommodate corneal birefringence is a dual-wavelength polarimetric system that takes advantage of the glucose dependency with wavelength depicted in Eq. (2).[5] The second method proposed by Cameron and Anumula is a dedicated birefringence compensator in conjunction with a single-wavelength polarimeter to directly subtract out birefringence.[11] In both cases, only *in vitro* results were obtained and, although each looked promising, neither approach attempted to quantify or understand the extent of the actual corneal birefringence. Thus, an improved quantification of this corneal birefringence through modeling would greatly facilitate the understanding of its effects on polarized light, and potentially help in the optimization of a polarimetric system for use in monitoring glucose in the eye.

Several theoretical and experimental eye models have been proposed to deal with the extent of birefringence.[12–17] Stanworth and Naylor proposed that the corneal birefringence for light passing normally though the cornea is small, but increases rapidly with increasing angle of incidence.[13] Bour and Lopes Cardozo proposed a method to measure the retardation as a function of the point of incidence on the pupil plane, and observed that corneal retardation has its slow axis along the tangent to the cornea, and that its magnitude increases with increasing eccentricity of the posterior corneal surface.[18] Van Blokland and Verhelst were one of the first to explain the polarization properties of the living human eye with a biaxial model.[14] They also hypothesized that for incidence at higher eccentricity (i.e., near the corneal limbus), a uniaxial model provides good approximation. More recently, Knighton, Huang, and Cavuoto mapped corneal birefringence using scanning laser polarimetry, and reported that a complete description of the corneal birefringence requires the cornea to be treated as a biaxial material.[17]

Most of this aforementioned research has been directed toward characterization of polarization properties of the eye, with a focus on ophthalmic imaging and diagnosis. Hence, the optical paths usually considered are limited to the region in the anterior chamber, which allow for light to pass through the pupil. The commercially available scanning laser polarimeters allow for polarization measurements, but are fundamentally limited to macular imaging. Several research groups have reported on the behavior of birefringence in the peripheral regions of cornea.[19–22] Misson utilized circular polarization biomicroscopy to study corneal structure and birefringence.[19] Jaronski and Kasprzak devised a phase stepping imaging polarimetry technique to measure the birefringence of human cornea *in vitro*, and concluded that corneal birefringence increases monotonically in the direction of the corneal periphery.[20,23] Hitzenberger, Gotzinger and Pircher employed polarization sensitive optical coherence tomography to map the distribution of birefringence at the posterior corneal surface.[21] Their results indicated that birefringence is low for beams incident normal to the corneal surface, and that at oblique angles, measured birefringence increases with deviation from normal incidence. These mentioned reports show the behavior of birefringence in the corneal periphery, and are similar in that the direction of beam incidence is always taken to be normal or near normal to the center of the cornea. Our group has developed a coupling mechanism to index match the eye and allow light to pass across the anterior chamber of the eye.[2] This setup uses mirrors and an inverted tube filled with saline solution as index-matching fluid between air and cornea to provide a straight path across the anterior chamber, with no coupling through the pupil. Thus, in this work a theoretical model is developed for index-matched light coupling in the eye to understand the effect of corneal birefringence on polarimetric quantification of glucose as light is passed across the eye, starting from the apex to the limbus, as depicted in Fig. 1.

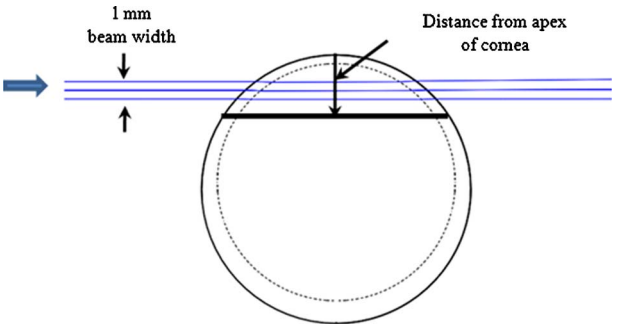

Fig. 1 Optical path through the anterior chamber of the eye. Note that the beam passes effectively straight through the chamber due to the assumption that the eye is index matched.

2 Materials and Methods

All optical modeling and calculations were performed in Code V (Optical Research Associates, Pasadena, California) optical design software package and Matlab (The MathWorks, Natick, Massachusetts). The physical parameters of the anterior chamber of the eye were taken from Ref. 24, in which the corneal surfaces are treated as spheres. Although a more accurate description of an eye model would include corneal surfaces to be treated as aspherics, the focus of our study was to model the corneal birefringence and not the exact anatomical dimensions, which are necessary for imaging models. Moreover, it has been shown that an asperical representation of the corneal surface results in a thinner cornea near the limbus when compared to our spherical model.[25] This will result in a smaller optical path through the cornea and hence have a smaller effective birefringence. Thus, we believe that our spherical eye model represents the worst case scenario, where the corneal thickness near the limbus is greater than that of an anatomically accurate eye model. As shown in Fig. 2, the anterior and posterior sides of the cornea were modeled as spherical surfaces centered at the optical axis of the eye with radii of 7.7 and 6.8 mm, respectively. Corneal thickness at the center was 0.5 mm, gradually increasing with eccentricity of the corneal surface. The refractive indices of cornea and aque-

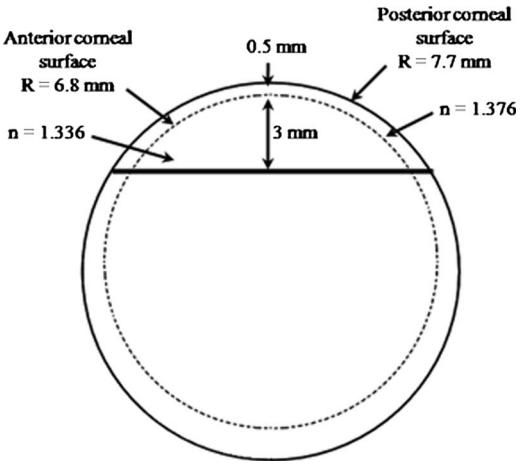

Fig. 2 Representative dimensions of the human eye model.

ous humor were taken to be 1.376 and 1.336, respectively. The environment outside the posterior corneal surface was assumed to be buffered aqueous-saline solution ($n=1.33$) for index matching.

A local $x-y-z$ coordinate system is defined at any arbitrary point on the posterior corneal surface such that the tangential plane at that point coincides with the $x-y$ plane, then the fast axis points in the z direction, as illustrated in Fig. 3. Hence, the electric field of a light ray incident normal to the corneal surface only experiences n_x and n_y. In general, not all incident light is normal to the cornea, and therefore, the corresponding electric field vector experiences n_x, n_y, and n_z. Thus, a biaxial model can better explain the corneal birefringence, in which each of the principle coordinate axes is associated with a different refractive index. However, according to Van Blokland and Verhelst, n_z-n_y is about 10 times larger than n_y-n_x.[14] Therefore, at larger oblique incident angles (as proposed for our coupling scheme), a large component of the electric field vector lies along the z axis, and a uniaxial model will give a good approximation. We modeled our eye as a bent uniaxial slab, where at each point the fast axis coincides with the direction of local normal and a maximum birefringence of 0.00159, as calculated by Van Blokland and Verhelst.[14]

As shown in Fig. 1, incident light was laterally coupled to the anterior chamber of the eye. The advantage of using an index-matching solution is to minimize the change in the angle of refraction at the interface of solution and posterior corneal surface. This is due to the fact that the change in the refractive index between saline solution and cornea is on the order of 10^{-2}. Similarly, the same order of difference exists between refractive indices of cornea and aqueous humor, and hence the deviation in beam angle traversing through the eye is minimized. Moreover, a direct consequence of this minimal change in beam angle is that the output beam shape and size are retained along with negligible change in beam divergence. Due to the curvature of the cornea, the optical path length through the cornea, and thereby the retardance, varies greatly depending on the angle and point of incidence. To analyze and quantify this variation, in our eye model we initially assumed a circular light beam with a 635-nm wavelength and 1 mm diameter, and later used a 532-nm wavelength beam for comparison. Thus, to couple the full area of the beam, the topmost point of incidence was chosen to be 0.5 mm (radius of the beam) below the interior apex of the cornea. Similarly, the lowest point of incidence was chosen to be 0.5 mm above the corneal limbus. The polarization vector of light beam propagation model was chosen to be at 45 deg with the vertical axis to experience maximum change in the state of polarization and hence the worst-case condition.

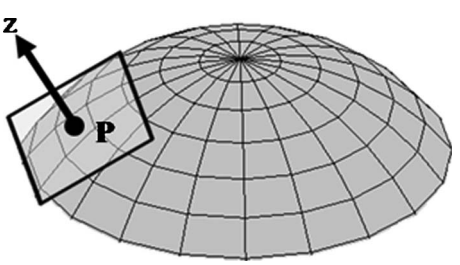

Fig. 3 Local coordinate system on the surface of the cornea at an arbitrary point P. The arrow signifies the normal (z axis) at that point, and the tangential plane at point P represents the $x-y$ plane.

3 Results and Discussion

To see the perceived change in angle of the polarization axis (or major axis for elliptically polarized output light) due to the corneal birefringence, the position of point of incidence was varied from top to bottom of the anterior chamber in 0.1-mm intervals. For this case, the glucose concentration in the aqueous humor was assumed to be zero, and hence it does not contribute to the rotation of light, but as described later on, the rotation for glucose across the anterior chamber even at the high concentration of 600 mg/dL still would be several times less (millidegrees) than the birefringence, and thus not visible on the graph in Fig. 4(a), which shows the angle of the major axis as a function of beam position. As depicted, there is a sharp change in angle near the apex, and the angle of the major axis switches by 90 deg across the circular state of polarization. It can be seen that the change in the perceived angle of polarization is much smaller for a beam position below 1 mm, and is minimal around 1.6 mm below the apex of cornea, which is near the center of the available probing line of incidence. Therefore, the effect of corneal birefringence can potentially be minimized for a beam incident roughly 1.6 mm below the apex of the eye. This can also be seen in Fig. 5, which shows the change in the shape of the polarizations ellipse as a function of beam position. The overall state of polarization of the output beam represents the average of the states of constituent rays across the full cross section of the beam. While the eccentricity of the ellipse changes in the center region around 1.6 mm below the apex of the eye, the orientation of the major axis stays relatively constant.

Apart from variation in birefringence, it is known from Eq. (1) that the optical path length through the aqueous humor of the eye and the glucose concentration itself would also change the measured rotation. Further, it is known that the path length is a function of beam position on the posterior corneal surface, and that the glucose level could vary across the physiologic range. Thus, both of these effects on the rotation should be quantified and compared to the changes observed

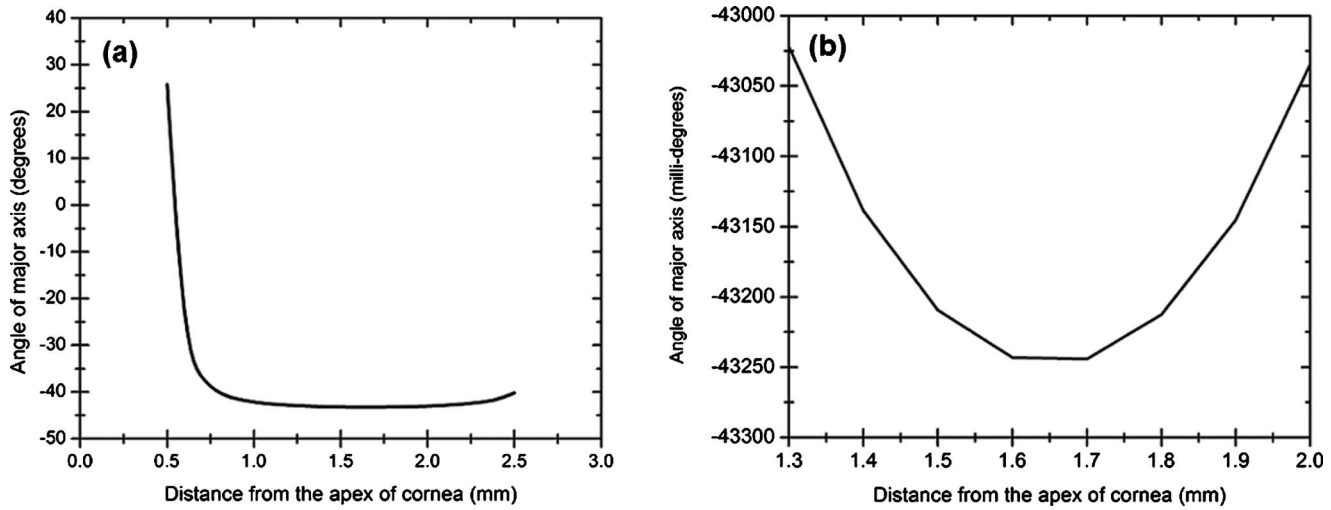

Fig. 4 (a) Angle of major axis of the output beam polarization ellipse as a function of distance from the apex of the cornea. Note that after a rapid change in the orientation of major axis near the apex, the variation is much smaller for beam positions below 1 mm. (b) Angle of major axis as a function of distance from apex of cornea—zoom-in view of the 1.3-mm to 2.0-mm region. Note that a shift in the beam position from 1.5 to 1.4 mm produces a net rotation of ~71 millideg due to change in corneal birefringence.

due to corneal birefringence. The change in optical path length as a function of the distance from the apex to the limbus is plotted in Fig. 6(a), and this is converted to a change in rotation as plotted in Fig. 6(b) using Eq. (1) and assuming a normal 100-mg/dL glucose concentration. The plot in Fig. 7 shows the change in rotation as a function of glucose concentration across the 0- to 600-mg/dL range for a beam position 1.6 mm below the apex, which corresponds to an optical path length of 8.82 mm. We also took into account the effect of glucose concentration-dependent change in the refractive index, and thereby, on the optical path length. The increase in the refractive index of an aqueous solution of glucose with increasing glucose concentration is 2.5×10^{-5}/mM glucose (or 1.39×10^{-6}/mg/dL).[26] This amounts to a change in refractive index of 8.34×10^{-4} across the physiologic glucose concentration range of 0 to 600 mg/dL. Such a small change in refractive index has negligible effect on beam path deviation across the physical path length in the anterior chamber of the eye.

It is evident from Figs. 3–7 that for any given change in beam position, such as that due to motion from respiration or other eye movements, the change in net rotation due to corneal birefringence is at least an order of magnitude larger than the effect of changes in optical path difference and aqueous humor glucose concentration. For instance, as depicted in Fig. 4(b), if the laser beam incidence shifts from 1.5 to 1.4 mm due to motion artifact, the change in the polarization vector due to corneal birefringence would be 70.8 millideg. In comparison, the corresponding change in optical path difference produces a net rotation of only 0.12 millideg. Similarly, a change in glucose concentration by ±10 mg/dL, which is approximately the current experimental error in glucose estimation,[5] changes the net rotation of polarization vector by ±0.4 millideg. This analysis clearly demonstrates that even in the most stable range, the time-varying corneal birefringence due to motion artifact is the most significant noise source in the sample and a major limitation preventing the realization of an optical polarimetric approach to ascertain

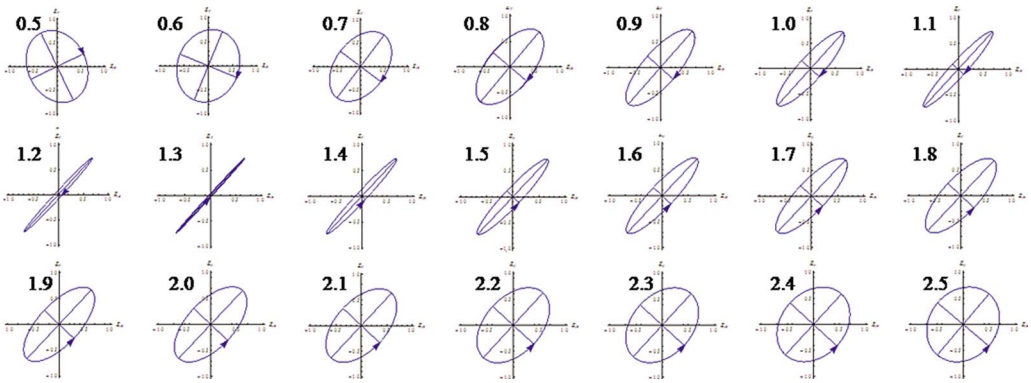

Fig. 5 Variation in state of polarization as a function of distance from the corneal apex. Note that although the eccentricity of the ellipse varies near the center of the eye, the major axis orientation stays relatively unchanged.

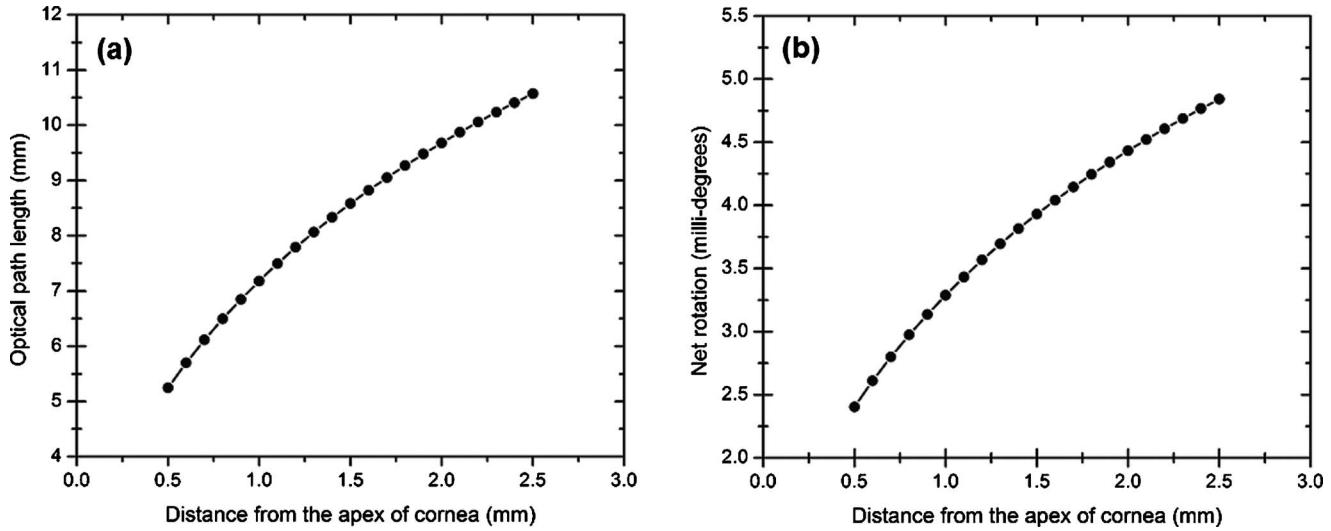

Fig. 6 (a) Change in optical path length through the aqueous humor as a function of distance from the apex of the cornea, and (b) corresponding net rotation in angle of polarization vector as a function of distance from the apex of the cornea.

aqueous humor glucose concentrations *in vivo*.

As mentioned, a possible method proposed by our group to reduce and potentially eliminate the effect of corneal birefringence is to utilize a multispectral scheme.[5,27,28] This is done by multiple-linear regression (MLR) analysis, which is analogous to scaled subtraction. By utilizing at least two wavelengths away from or between the absorption bands for glucose, MLR can accommodate the contribution of birefringence to the total rotation of the state of polarization, and Eq. (2) can be used to predict glucose. One of the assumptions for such an analysis is that the motion artifact is wavelength independent in the range of motion. To validate this assumption, we utilize a second wavelength away from the glucose absorption band at 532 nm, and examine the perceived angle of polarization axis due to corneal birefringence with respect to that of the 635-nm wavelength. Figure 8 shows the plot of major axes of elliptically polarized output beams at both wavelengths. It can be seen that after a rapid change near the apical region of the eye, the major axes orientations remain relatively unchanged and close to each other, especially between 1.4 and 1.8 mm. This observation leads to two important advantages. First, for any of the two wavelengths, coupling of light at just under the center of the cornea leads to minimum change in the state of output polarization due to motion artifact. Secondly, the major axis orientations of both wavelengths have similar magnitude, a direct consequence of which is that a dual-wavelength optical polarimeter can be utilized to reduce the sample noise associated with motion artifact.

Although the wavelength independence of corneal birefringence has been speculated earlier, and has been mainly attrib-

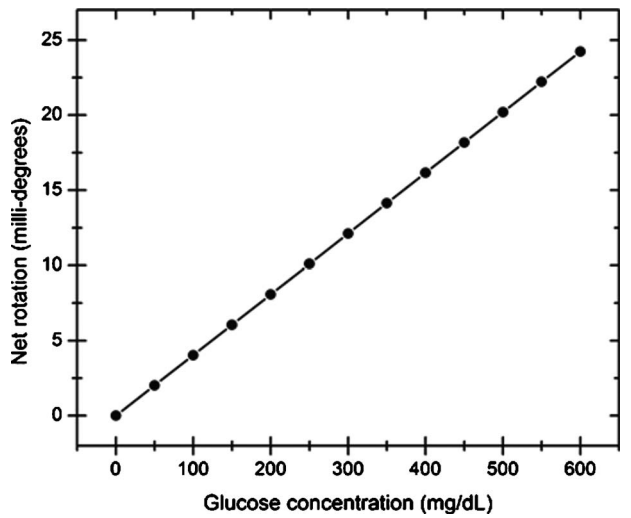

Fig. 7 Net rotation in the angle of polarization vector as a function of glucose concentration. The point of incidence is taken to be 1.6 mm below the corneal apex, which corresponds to an optical path length of 8.82 mm through the aqueous humor.

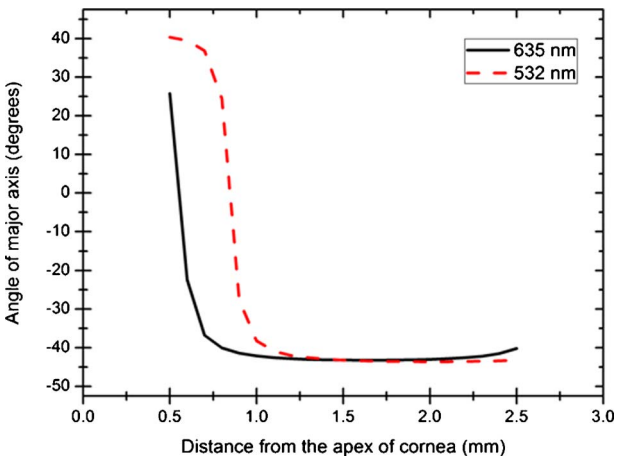

Fig. 8 Angle of major axes for wavelengths of 635 (solid line) and 532 nm (dashed line) as a function of distance from the apex of the cornea. Note that after a rapid change in the major axes orientations near the apex, the variation is much smaller for beam positions below 1 mm, and is of similar magnitude.

uted to the mechanism of form birefringence of corneal stroma,[29] the previous observation is unique due to the highly oblique incidence of the input light, and shows that the accommodation of corneal birefringence using the multiwavelength approach has validity for glucose monitoring. Further, the birefringence experienced at such eccentricities is an order of magnitude higher than that of normal incidence at the apical region of the cornea. Thus, the corneal birefringence models based on macular imaging are unlikely to measure the birefringence at corneal limbus, since the effective pupil size can vary greatly as a function of beam position.

4 Conclusion

In summary, a birefringent eye model for coupling index-matched light through the anterior chamber of the eye is presented. Corneal birefringence as a function of distance of the transmitted beam from the apex to the limbus of the index matched eye is shown to vary significantly, but is also shown to have a minimum in the region of 1.5 to 1.8 mm from the apex. The optical rotation is shown to vary as a function of optical path length, and the corneal birefringence as a function of point of incidence from apex to limbus. However, the variation in corneal birefringence with motion, even in the most stable region, manifests itself as the most significant source of noise (by at least an order of magnitude compared to path length or glucose concentration), which needs to be accommodated to realize a practical optical polarimeter for glucose sensing through the eye. The theoretical potential of a dual-wavelength polarimeter to minimize this sample noise from time-varying corneal birefringence due to motion artifact is shown. The next step in this study is to verify the results *in vivo* and to investigate possible mechanisms for unmatched refractive index coupling.

Acknowledgments

This work was supported by a grant from National Institutes of Health (R01 DK076772). The authors would like to acknowledge Optical Research Associates for providing the student license of CODE V software package.

References

1. B. D. Cameron, J. S. Baba, and G. L. Coté, "Measurement of the glucose transport time delay between the blood and aqueous humor of the eye for the eventual development of a noninvasive glucose sensor," *Diabetes Technol. Ther.* **3**(2), 201–207 (2001).
2. B. D. Cameron, H. W. Gorde, B. Satheesan, and G. L. Coté, "The use of polarized laser light through the eye for noninvasive glucose monitoring," *Diabetes Technol. Ther.* **1**(2), 135–143 (1999).
3. B. Rabinovitch, W. F. March, and R. L. Adams, "Noninvasive glucose monitoring of the aqueous humor of the eye: part I. Measurement of very small optical rotations," *Diabetes Care* **5**(3), 254–258 (1982).
4. B. D. Cameron and G. L. Coté, "Noninvasive glucose sensing utilizing a digital closed-loop polarimetric approach," *IEEE Trans. Biomed. Eng.* **44**(12), 1221–1227 (1997).
5. B. H. Malik and G. L. Coté, "Real-time, closed-loop dual-wavelength optical polarimetry for glucose monitoring," *J. Biomed. Opt.* **15**(1), 017002 (2010).
6. T. W. King, G. L. Coté, R. McNichols, and M. J. Goetz, Jr, "Multispectral polarimetric glucose detection using a single Pockels cell," *Opt. Eng.* **33**(8), 2746–2753 (1994).
7. D. J. Donohue, B. J. Stoyanov, R. L. McCally, and R. A. Farrell, "Numerical modeling of the cornea's lamellar structure and birefringence properties," *J. Opt. Soc. Am. A* **12**(7), 1425–1438 (1995).
8. M. Born and E. Wolf, *Principles of Optics*, Cambridge University Press, Oxford, UK (1999).
9. R. A. Farrell, D. Rouseff, and R. L. McCally, "Propagation of polarized light through two- and three-layer anisotropic stacks," *J. Opt. Soc. Am. A* **22**(9), 1981–1992 (2005).
10. F. C. a. P. Salvadori, Ed., *Fundamental Aspects and Recent Developments in Optical Rotatory Dispersion and Circular Dichroism*, Heyden and Son Ltd., London (1973).
11. B. D. Cameron and H. Anumula, "Development of a real-time corneal birefringence compensated glucose sensing polarimeter," *Diabetes Technol. Ther.* **8**(2), 156–164 (2006).
12. A. Stanworth and E. J. Naylor, "Polarized light studies of the cornea," *J. Exp. Biol.* **30**, 160–163 (1953).
13. A. Stanworth and E. J. Naylor, "The polarization optics of the isolated cornea," *Br. J. Ophthamol.* **34**, 201–211 (1950).
14. G. J. Van Blokland and S. C. Verhelst, "Corneal polarization in the living human eye explained with a biaxial model," *J. Opt. Soc. Am. A* **4**(1), 82–90 (1987).
15. J. S. Baba, B. D. Cameron, S. Theru, and G. L. Coté, "Effect of temperature, pH, and corneal birefringence on polarimetric glucose monitoring in the eye," *J. Biomed. Opt.* **7**(3), 321–328 (2002).
16. R. W. Knighton and X. R. Huang, "Linear birefringence of the central human cornea," *Invest. Ophthalmol. Visual Sci.* **43**(1), 82–86 (2002).
17. R. W. Knighton, X. R. Huang, and L. A. Cavuoto, "Corneal birefringence mapped by scanning laser polarimetry," *Opt. Express* **16**(18), 13738–13751 (2008).
18. L. J. Bour and N. J. Lopes Cardozo, "On the birefringence of the living human eye," *Vision Res.* **21**(9), 1413–1421 (1981).
19. G. P. Misson, "Circular polarization biomicroscopy: a method for determining human corneal stromal lamellar organization *in vivo*," *Ophthalmic Physiol. Opt.* **27**(3), 256–264 (2007).
20. J. W. Jaronski and H. T. Kasprzak, "Linear birefringence measurements of the *in vitro* human cornea," *Ophthalmic Physiol. Opt.* **23**(4), 361–369 (2003).
21. C. K. Hitzenberger, E. Gotzinger, and M. Pircher, "Birefringence properties of the human cornea measured with polarization sensitive optical coherence tomography," *Bull. Soc. Belge Ophtalmol* **302**, 153–168 (2006).
22. J. M. Bueno and F. Vargas-Martín, "Measurements of the corneal birefringence with a liquid-crystal imaging polariscope," *Appl. Opt.* **41**(1), 116–124 (2002).
23. J. W. Jaronski and H. T. Kasprzak, "Generalized algorithm for photoelastic measurements based on phase-stepping imaging polarimetry," *Appl. Opt.* **38**(34), 7018–7025 (1999).
24. D. Atchison and G. Smith, *Optics of the Human Eye*, Butterworth Heinemann, Oxford, UK (2000).
25. H. L. Liou and N. A. Brennan, "Anatomically accurate, finite model eye for optical modeling," *J. Opt. Soc. Am. A* **14**(8), 1684–1695 (1997).
26. R. C. Weast, Ed., *Handbook of Chemistry and Physics*, CRC Press, Cleveland, OH (1974).
27. Q. Wan, G. L. Coté, and J. B. Dixon, "Dual-wavelength polarimetry for monitoring glucose in the presence of varying birefringence," *J. Biomed. Opt.* **10**(2), 024029 (2005).
28. B. H. Malik and G. L. Coté, "Real-time dual wavelength polarimetry for glucose sensing," *Proc. SPIE* **7186**, 718604 (2009).
29. W. N. Charman, Ed., *Visual Optics and Instrumentation*, CRC Press, Boca Raton, FL (1991).